

1 **Development of HILIC-MS/MS method for acyl-CoAs covering** 2 **short- to long-chain species in a single analytical run**

3 Madhulika Singh¹, Ligia Akemi Kiyuna², Christoff Odendaal², Barbara M. Bakker², Amy C.
4 Harms¹, Thomas Hankemeier^{1*}

5 ¹Metabolomics and Analytics Centre, Leiden Academic Centre for Drug Research,
6 Leiden University, The Netherlands

7 ²University of Groningen, University Medical Center Groningen, Groningen, The Netherlands

8
9 (*) Corresponding author:

10 Thomas Hankemeier

11 Einsteinweg 55, 2333 CC Leiden, The Netherlands

12 Tel.: +31 71 527 1340

13 E-mail: hankemeier@lacdr.leidenuniv.nl

14 15 **Abstract**

16 Acyl-CoAs play a significant role in numerous physiological and metabolic processes making
17 it important to assess their concentration levels for evaluating metabolic health. Considering
18 the important role of acyl-CoAs, it is crucial to develop an analytical method that can analyze
19 these compounds. Due to the structural variations of acyl-CoAs, multiple analytical methods
20 are often required for comprehensive analysis of these compounds, which increases complexity
21 and the analysis time. In this study, we have developed a method using a zwitterionic HILIC
22 column that enables the coverage of free CoA and short- to long-chain acyl-CoA species in one
23 analytical run. Initially, we developed the method on a QTOF instrument for the identification
24 of acyl-CoA species, optimizing their chromatography and retention times. Later, a targeted
25 HILIC-MS/MS method was created in scheduled multiple reaction monitoring mode on a
26 QTRAP instrument. The performance of the method was evaluated based on various parameters
27 such as linearity, precision, recovery and matrix effect. This method was applied to identify the
28 difference in acyl-CoA profiles in HepG2 cells cultured in different conditions. Our findings
29 revealed an increase in levels of acetyl-CoA, medium- and long-chain acyl-CoA while a
30 decrease in the profiles of free CoA in the starved state, indicating a clear alteration in the fatty
31 acid oxidation process.

32 33 **Keywords**

34 Acyl-CoA, LC-MS, HILIC, HepG2, FAOD, Biomarker

35

36 1. Introduction

37 Acyl-CoAs are thioester compounds that have a pivotal role in various metabolic processes
38 such as fatty acid beta-oxidation, biosynthesis of lipids, signaling, and xenobiotics metabolism
39 [1,2]. The most important biological function of acyl-CoAs is in the metabolism of fatty acids
40 via beta-oxidation. The fatty acid beta-oxidation (FAO) process in the liver breaks down fatty
41 acids (FA) to produce adenosine triphosphate (ATP) in low glucose conditions[3,4]. Acyl-CoAs
42 are formed when a FA forms a thioester bond with Coenzyme-A (CoA)[5,6]. These acyl-CoAs
43 are transported inside the mitochondria for the entire process of FAO. Fatty acid oxidation
44 disorders (FAOD) occur due to the deficient activity of the enzymes or transporter proteins
45 involved in the pathway, which results in the accumulation of acyl-CoA esters[3]. The acyl-
46 CoA accumulation profile provides information on the type of fatty acid oxidation disorder
47 (FAOD). Intracellular acyl-CoA levels are important reporters of metabolic health and their
48 accumulation in case of FAOD makes them interesting biomarkers[7]. Apart from FAOD,
49 these compounds are also involved in progression of cancer[8–10], diabetes[11–14], precursors
50 for lipid synthesis and ketone bodies. Since acyl-CoA are involved in numerous physiological
51 and pathophysiological pathways, it is important to develop analytical methods for their
52 identification and quantification.

53 Developing chromatographic methods for acyl-CoAs is challenging due to their structural
54 complexity. These compounds exhibit significant variations in their physicochemical properties
55 by factors such as carbon chain length, degree of saturation, and the presence of functional
56 groups[15–17]. Additionally, acyl-CoAs have low endogenous levels and are highly unstable
57 in aqueous solutions. Due to these reasons they are susceptible to hydrolysis, making sample
58 preparation challenging and resulting in poor recovery and low signal intensity[15,18]. The
59 quantification of acyl-CoAs has previously been accomplished using a variety of analytical
60 techniques, such as gas chromatography, capillary electrophoresis, and reversed phase liquid
61 chromatography (RP-LC) coupled to UV or fluorescence detection[19–22]. However, liquid
62 chromatography coupled to mass spectrometry (LC-MS), is the most widely used technique for
63 acyl-CoA analysis due to its higher sensitivity and selectivity. On the other hand, severe peak
64 tailing, signal deterioration, and poor detection limits are common obstacles associated with
65 this approach[23,24]. Various efforts have been made to cover the full range of acyl-CoA in a
66 single analytical run. One such method is to use ion-pairing reagents such as triethylamine[25]
67 or dimethylbutyl amine[16,26]. However, ion-pairing reagents are reported to decrease mass
68 spectrometry signal intensity[27] and frequent cleaning of detectors is required. Another

69 approach is to use two-dimensional(2D)LC-MS[17], but the complexity and analysis time are
70 increased by inclusion of a second dimension of separation, which has an impact on throughput.
71 Furthermore, a RP-LC-MS/MS technique based on phosphate methylation after acyl-CoA
72 derivatization has been reported[15]. Nonetheless, derivatization complicates sample
73 preparation and requires investigation for the evaluation of complete chemical conversion.
74 Hydrophilic interaction liquid chromatography (HILIC) has become increasingly popular and
75 promising for the separation of polar compounds, as HILIC allows class-based separation by
76 hydrophilic interaction. Despite significant variations in chain length polarity, the presence of
77 a similar hydrophilic headgroup in acyl-CoAs facilitates their elution within a relatively shorter
78 time period. In HILIC chromatography, the compounds are separated on a polar stationary
79 phase by gradually increasing solvent polarity[28–30]. The compounds with higher polarity
80 have enhanced affinity for the polar stationary phase, thus resulting in prolonged retention,
81 whereas compounds with lower polarity tend to elute earlier.
82 The aim of the present study is to develop a targeted HILIC-MS/MS method utilizing a
83 zwitterionic HILIC column for the quantification of free CoA and short- to long-chain acyl-
84 CoA compounds in a single analytical run (covering the full analyte range from high to low
85 polarity) and demonstrate the utility of this method in HepG2 cell application. To achieve this,
86 the initial method development was done on a high-resolution QTOF instrument (HRMS) for
87 pre-screening of species and identifying their retention time. The chromatography was
88 optimized by studying the effects of different factors such as buffer concentration and injection
89 solvents, to obtain the satisfactory peak shape. After optimization of various LC-MS settings,
90 a targeted method was created and validation parameters such as linearity, sensitivity, precision,
91 recovery and matrix effect were examined to evaluate method performance in the HepG2 cells.
92 Finally, the HILIC-MS/MS method was applied to compare the free CoA and acyl-CoA profile
93 in HepG2 cells cultured in different conditions.

94 95 **2. Materials and methods**

96 97 *2.1. Chemicals and reagents*

98 Analytical grade solvents including acetonitrile, chloroform, dichloromethane, isopropanol
99 (IPA) and methanol (MeOH) were purchased from Biosolve BV (Valkenswaard, The
100 Netherlands). Purified water was obtained using the Milli-Q Advantage A10 Water Purification
101 System manufactured by Merck Millipore (Billerica, MA, USA). Ammonium acetate with a
102 purity of 99% was supplied by Sigma-Aldrich (St. Louis, MO, USA). Acyl-CoA standards,
103 such as acetyl-CoA (C2:0-CoA) and propionyl-CoA (C3:0-CoA) as sodium salts, octanoyl-

104 CoA (C8:0-CoA), pentadecanoyl-CoA (C15:0-CoA), palmitoyl-CoA (C16:0-CoA),
105 heptadecanoyl-CoA (C17:0-CoA), and 11Z-octadecenoyl-CoA (C18:1(n7)-CoA) as
106 ammonium salts, were purchased from Avanti Polar Lipids (Alabaster, AL, USA). Acetyl-1,2-
107 ¹³C₂-CoA (C2:0(¹³C₂)-CoA) and n-heptanoyl-CoA (C7:0-CoA) in the form of lithium salts were
108 obtained from Sigma-Aldrich (St. Louis, MO, USA). Additional acyl-CoA standards, including
109 free CoA (CoA), butyryl-CoA (C4:0), hexanoyl-CoA (C6:0), octanoyl-CoA (C8:0), decanoyl-
110 CoA (C10:0), lauroyl-CoA (C12:0), myristoyl-CoA (C14:0), palmitoyl-CoA (C16:0), and
111 stearoyl-CoA (C18:0), were provided by collaborators at UMCG (Groningen, The
112 Netherlands).

113 Dulbecco's Modified Eagle Medium (DMEM) (Product No. P04-01500) and glucose-free
114 DMEM (Product No. P04-01548S1) was purchased from PAN Biotech™. Fetal bovine serum
115 (FBS) and Phosphate-buffered saline (PBS) were purchased from Gibco while L-carnitine
116 (Product No. C0283) and palmitate (Product No. P9767) were purchased from Sigma-Aldrich.
117

118 2.2. Cell culture

119 Wildtype HepG2 cells were maintained in DMEM with 5 mM glucose, 3.7 g L⁻¹ NaHCO₃, 1
120 mM sodium pyruvate and amino acids, supplemented with 3 mM glutamine, and 10% FBS.
121 The cells were kept at 37°C and 5% CO₂. To test the individual and combined effects of glucose
122 depletion and fatty acid stimulation on the free CoA level and acyl-CoA profile, the cells were
123 incubated for 24 hours in two different conditions. In condition 1 the cells were cultured in
124 DMEM (5 mM glucose, 1 mM pyruvate supplemented with 3 mM glutamine and 10% FBS)
125 with additional supplements 2 mM L-carnitine and 0.5 mM BSA-bound palmitate. Condition 2
126 was with glucose-free DMEM (no glucose, no glutamine, no pyruvate, 10% FBS) supplemented
127 with 2 mM L-carnitine and 0.5 mM BSA-bound palmitate. After 24 hours, the cells were
128 washed twice with ice-cold PBS and harvested for further analysis. Condition 1 cells were
129 "supplemented cells" with multiple carbon sources, while condition 2 cells were "starved cells"
130 with fewer carbon sources.

131

132 2.3. Sample preparation

133 HepG2 cells were extracted by a two-step protocol using chloroform/methanol/water based on
134 the Bligh and Dyer approach[31]. 10 µL of acyl-CoA internal standard (IS) containing mixture
135 of C2:0(¹³C₂)-CoA, C7:0-CoA, C15:0-CoA and C17:0-CoA with concentration of 3 µM were
136 spiked in the HepG2 cell extracts containing 1×10⁶ cells in 100 µL of methanol. To this extract,
137 220 µL of cold methanol and 100 µL of cold water was added and sonicated for 3 min. After

138 sonication, 320 μ L of chloroform and 188 μ L of water were added. Samples were vortexed for
139 1 minute, left to partition on ice for 10 minutes, and centrifuged at 15800 rcf for 15 minutes at
140 4 °C. 450 μ L of the upper aqueous layer was transferred to a new Eppendorf tube. Samples
141 were evaporated to dryness with a Labconco CentriVap vacuum concentrator (Kansas City,
142 MO, USA). The dried samples were reconstituted in 100 μ L of methanol/water/isopropanol
143 (1:1:1), and transferred to HPLC vial for LC-MS analysis.

144

145 *2.4. HILIC-HRMS (HILIC-MS) analysis*

146 The Waters Synapt G2-S quadrupole time-of-flight mass spectrometer with an electrospray
147 ionization (ESI) source (Milford, MA, USA) was coupled to an Acquity UPLC system
148 (Waters). The chromatographic separation was performed on SeQuant® ZIC®-cHILIC HPLC
149 (100 mm x 2.1 mm, 100 Å pore size, 3 μ m) column. The column oven and autosampler
150 temperatures were set at 40 °C and 10 °C respectively. Mobile phase A (MPA) consisted of
151 acetonitrile:water (9:1) containing 5 mM ammonium acetate and acetonitrile:water (1:9) with
152 5 mM ammonium acetate was used for mobile phase B (MPB). The flow rate was 0.25 mL/min
153 and injection volume was 5 μ L. The gradient elution is shown in **Table S1**. The autosampler
154 injection needle was washed with a weak needle wash consisting of acetonitrile:water (1:9, v/v)
155 and strong needle wash consisting of acetonitrile:water (9:1, v/v).

156 For the MS analysis, a time-of-flight (TOF) MS scan was performed. The mass spectrometer
157 was set to scan a mass range from 300 to 1200 Da in both positive and negative electrospray
158 (ESI) ionization modes. To ensure accurate mass measurement, 0.1 mg/L leucine-enkephalin
159 in water:MeOH:formic acid (50:50:0.1, v/v/v) was used as a lock-mass calibrant with the
160 infusion flow rate of 10 μ L/min. The mass spectrometer was operated with the following
161 parameters: the capillary voltage was set at 2.50 kV in both positive and negative mode of
162 ionization; the sampling cone voltage was set to 30 V and the source offset voltage was 100 V.
163 The source temperature was maintained at 125°C, while the desolvation temperature was set at
164 500°C. Gas flows were controlled as follows: the cone gas flow rate was set to 50 L/h; the
165 desolvation gas flow rate was 500 L/h, and the nebulizer gas flow rate was adjusted to 6 Bar.

166

167 *2.5. HILIC-QTRAP (HILIC-MS/MS) analysis in scheduled MRM mode*

168 The targeted HILIC-MS/MS analysis was performed on a Waters Acquity UPLC I-class system
169 from Waters (Milford, MA, USA) coupled to an AB Sciex QTRAP 6500 mass spectrometer
170 (Concord, ON, Canada). The needle wash was acetonitrile:water (1:1, v/v). The column, mobile

171 phase, autosampler temperature and column oven temperature were the same as described in
172 section 2.4. with a slight modification in the gradient as shown in **Table 1**.

173 **Table 1.** Gradient for HILIC-MS/MS analysis.

Time (min)	Flow rate (mL min⁻¹)	MP-A (%)	MP-B (%)
Initial	0.25	95	5
2.3	0.25	95	5
8.5	0.25	25	75
13.00	0.25	15	85
15.5	0.25	15	85
15.6	0.25	95	5
20	0.25	95	5

174
175 The MS/MS experiments were conducted on a Turbo V source. The analysis was conducted in
176 positive ion mode and analytes were monitored in scheduled multiple reaction monitoring
177 (sMRM) mode. The mass spectrometer was operated at the following settings: the curtain gas
178 (N₂) pressure was set to 25 psi, and the collision gas (N₂) was maintained at a medium level.
179 The spray voltage was set at 4000 V in positive ion mode. The source temperature was
180 maintained at 325 °C. The GS1 and GS2 pressures both were set at 60 psi. The target scan time
181 was of 0.35 sec. The delustering potential (DP) and collision energy (CE) were optimized to
182 achieve maximum response.

183 184 *2.6. Method validation*

185 Method validation of the HILIC-MS/MS method was performed using non-endogenous acyl-
186 CoA standards- C2:0(¹³C₂)-CoA, C7:0-CoA, C15:0-CoA, and C17:0-CoA. These standards
187 were either isotopically labeled or had odd chains to be free from interference from endogenous
188 species.

189 190 *2.6.1. Calibration curves*

191 The calibration curves were freshly prepared on three different days to assess the linearity of
192 the method. For this purpose, an 8-point calibration line was created by serially diluting the
193 standards. The concentrations of these calibration points are presented in **Table S2**. Three types
194 of calibration lines were prepared: 1) Neat solvents; 2) Spiking standards in HepG2 cells before
195 performing the extraction as described in the sample preparation section; 3) Spiking standards

196 in HepG2 cells after extraction. To determine the linear range, an unweighted linear regression
197 model was employed. The calculation of various validation parameters was performed using
198 cal-3 (low), cal-5 (medium), and cal-7 (high) concentration levels.

199

200 2.6.2. Limit of detection (LOD) and Lower limit of quantitation (LLOQ)

201 LOD and LLOQ were calculated by using equation 1 and equation 2 respectively.

202

$$203 \quad LOD = \frac{3 \times SD_{area_{C_{S/N>3}}} + area_{blank}}{\frac{area_{C_{S/N>3}}}{[C_{S/N>3}]}} \quad (1)$$

$$204 \quad LLOQ = \frac{10 \times SD_{area_{C_{S/N>3}}} + area_{blank}}{\frac{area_{C_{S/N>3}}}{[C_{S/N>3}]}} \quad (2)$$

205

206 where $SD_{area_{C_{S/N>3}}}$ represents the standard deviation of area of the lowest concentration with
207 signal to noise ratio greater than $3(C_{S/N>3})$, $area_{blank}$ are the peak area of the blank and

208 $\frac{area_{C_{S/N>3}}}{[C_{S/N>3}]}$ represents the ratio between peak area and concentration at $C_{S/N>3}$ [32].

209

210 2.6.3. Precision

211 Precision was assessed by calculating the relative standard deviation (RSD %). Low, medium
212 and high concentration levels were used for this analysis. Intraday precision was determined by
213 conducting three consecutive measurements on the same day. Interday precision, on the other
214 hand, was evaluated by measuring the samples on three different days. The precision was
215 calculated by equation 3 [33].

$$216 \quad RSD (\%) = \frac{Standard\ deviation}{Mean} \times 100 \quad (3)$$

217

218 2.6.4. Extraction Recovery

219 The response of standards at low, medium and high levels (measured in triplicate) was
220 calculated in the samples spiked before and after extraction in HepG2 cells and equation 4 was
221 used to calculate the recovery.

$$222 \quad Recovery(\%) = \frac{Response\ of\ standards\ in\ HepG2\ cells\ before\ extraction}{Response\ of\ standards\ in\ HepG2\ cells\ after\ extraction} \times 100 \quad (4)$$

223

224 2.6.5. Matrix effect

225 Matrix effect is a prevalent issue encountered in mass spectrometry measurements. It refers to
226 a phenomenon where the response of an analyte is suppressed or amplified due to the presence

227 of a matrix or other interfering components that affect the ionization process of compounds.
228 This was calculated with equation 5 at low, medium and high level (measured in triplicate).

229
230
$$\text{Matrix effect(\%)} = \frac{\text{Response of standards in HepG2 cells after extraction}}{\text{Response of standards in neat solvents}} \times 100 \quad (5)$$

231
232

233 2.6.6. Carryover

234 Carryover refers to the presence of analytes in the blank samples after injection of the highest
235 calibration standards[34]. This was evaluated by comparing the peak area of standards in the
236 blank solvents to the peak area of standards spiked in high concentration in HepG2 cells,
237 analyzed before the blank solvents.

238 2.6.7. Repeatability

239 The repeatability of our method was assessed by calculating RSD (%) of endogenous acyl-CoA
240 species in the quality control (QC) samples inserted at regular intervals in the batch of study
241 samples.
242

243 2.7. Quantitation

244 The odd-chain or isotopic labeled non-endogenous standards were used as internal standards
245 for the quantitation of endogenous acyl-CoA species. C2:0(¹³C₂)-CoA was used for the
246 quantitation of short-chain species, C7:0-CoA was used for the quantitation of medium-chain
247 species while C15:0-CoA and C17:0-CoA were used for the quantitation of long-chain species.
248 These standards were used for the quantitation of both saturated and unsaturated species. In this
249 study, we find that the abundance of unsaturated species in the biological samples was very low
250 and hence their contribution to isotopic interference was less than 1%. Therefore, we do not
251 require any isotopic correction in this study.
252

253 2.8. Data processing

254 Data acquisition was performed using MassLynx (version 4.1) for the Synapt G2-S (HILIC-
255 MS) and Analyst (version, 1.6.2) for the QTRAP (HILIC-MS/MS). Peak integration was
256 performed using TargetLynx (version 4.1) and Sciex OS (version 2.1.6) for HILIC-MS and
257 HILIC-MS/MS respectively. The peak asymmetry factor was used to determine the effect of
258 different conditions during method development and was calculated by equation 6[35].
259

260
$$A_s = b/a \quad (6)$$

261 where A_s = peak asymmetry factor, b = half width of peak (distance from peak midpoint to the
262 trailing edge at 10% of the full peak height), a = front half width (distance from peak midpoint
263 to leading edge at 10% of the peak height). A_s is lower than 1 for a fronting peak and higher
264 than 1 for a tailing peak.

265 GraphPad Prism (version 9) was used to calculate statistical significance between the groups
266 using t-test and plot graphs.

267 **3. Results and Discussion**

268 Representative standards C2:0-CoA (short-chain), C8:0-CoA (medium-chain), C16:0-CoA
269 and C18:1-CoA (long-chain) from each chain-length was used for method optimization.

270

271 *3.1 Mass spectrometry parameters optimization*

272 The TOF MS scan on the Synapt G2-S was performed in both positive ESI mode (ESI⁺) and
273 negative ESI (ESI⁻) mode by injecting a mixture of four representative acyl-CoA standards.
274 Firstly, the observed mass of the representative standards were confirmed with their accurate
275 masses in protonated [M+H]⁺, deprotonated [M-H]⁻ and doubly charged negative ions [M-2H]²⁻
276 form. The corresponding m/z values of these acyl-CoA standards are presented in **Table S3** and
277 sensitivity of acyl-CoA standards in different ionization modes is shown in **Figure S1**. Doubly
278 charged ions in the negative mode [M-2H]²⁻ have slightly higher sensitivity for these standards
279 compared to their protonated form [M+H]⁺ while intensities were very low in singly negative
280 charged ion [M-H]⁻. Despite the slightly higher sensitivity observed in the doubly charged ions
281 in negative mode, we decided to measure protonated species utilizing positive ionization mode
282 for our analysis. This choice was based on the previously reported studies[16–18] and the
283 fragmentation observed in positive ionization mode offers a more straightforward pattern for
284 acyl-CoA analysis. **Table S4** presents the observed m/z of all the targets with their identified
285 retention time in the HRMS method.

286

287 *3.2 Chromatographic separation for acyl-CoAs*

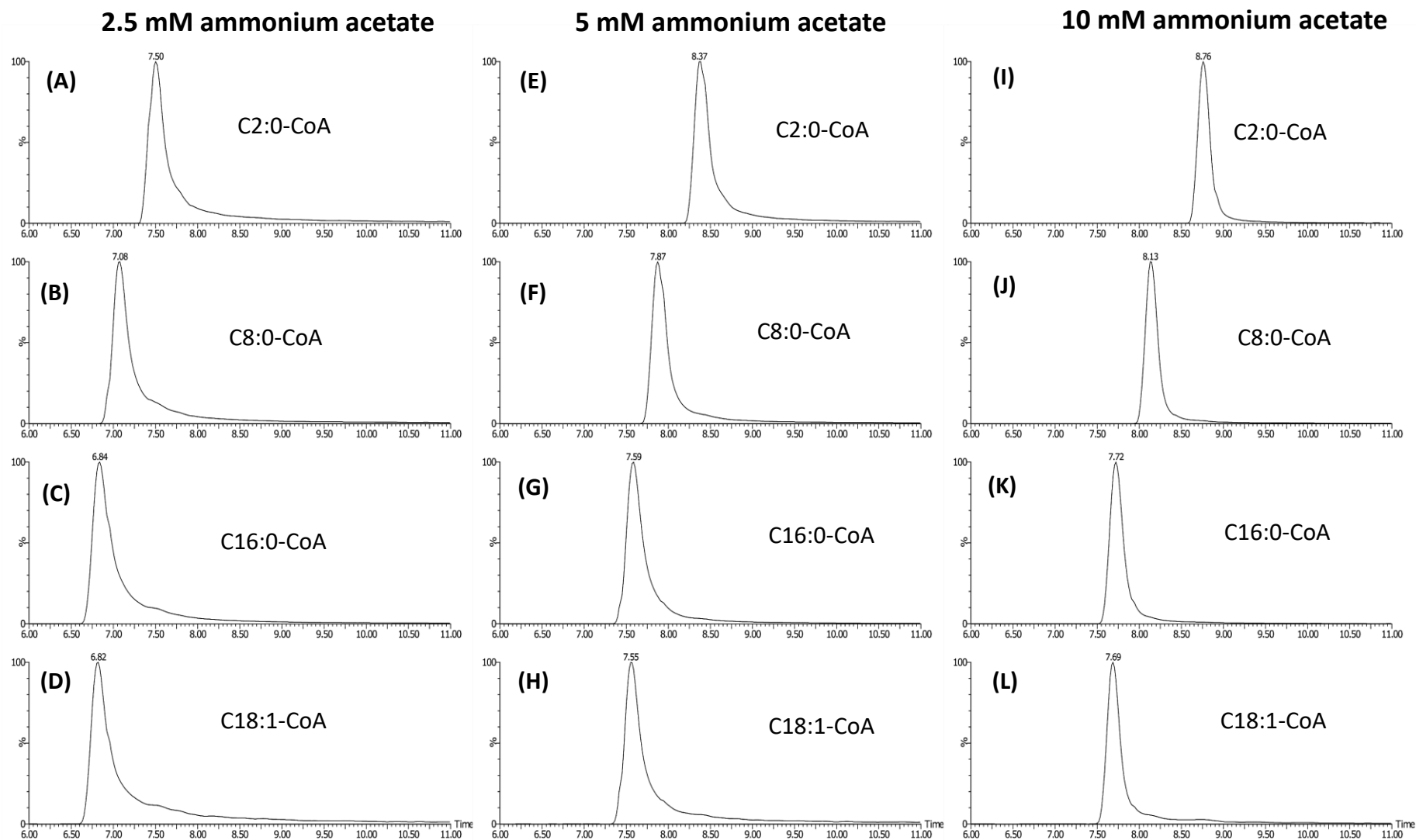
288 We started the chromatographic separation with a 20 min gradient as reported in section **Table**
289 **S1**. In order to achieve the quantification of all acyl-CoA species in a single analytical run, we
290 employed a ZIC-chILIC column which contains a phosphorylcholine group (**Figure S2**) that
291 consists of a negatively charged inner moiety and a positively charged outer moiety[36]. We
292 chose to use this ZIC-chILIC column for the chromatography optimization of acyl-CoA as it
293 was reported to effectively separate various compounds containing phosphate groups like ATP,

294 ADP, NAD, sugar phosphates, etc.[37–39]. The presence of a zwitterionic stationary phase
295 requires lower concentrations of buffer compared to other types of stationary phases, as the
296 zwitterionic stationary phase contains both positive and negative charges. This causes weak
297 electrostatic interactions with the analytes and hence only a low concentration of buffer is
298 needed[36]. The peak tailing observed in the acyl-CoA species can be attributed to the presence
299 of the phosphate group on CoA moiety[40]. This phenomenon occurs due to the strong
300 interaction between the phosphate group and specific sites within the column. Additionally,
301 these phosphate groups have a tendency to adhere to the stainless parts of the LC-MS
302 instrumentation, further contributing to the challenges in analysis[40]. The buffer salts such as
303 ammonium acetate and ammonium formate etc., are known to maintain the ionization of
304 analytes and decrease the interaction between stationary phase and analytes[28,41–43]. We
305 have used ammonium acetate buffer as this is one of the most commonly used buffers for
306 metabolomics studies employing HILIC chromatography[42–44]. In this study, we investigated
307 the impact of different concentrations of ammonium acetate on the peak shape, separation and
308 retention of acyl-CoAs. Mobile phases were prepared with concentrations of 2.5 mM, 5 mM,
309 and 10 mM ammonium acetate and the buffer concentration was kept same in both mobile
310 phases to maintain consistent ionic strength throughout the gradient elution. **Figure 1** displays
311 the peaks of the acyl-CoA standards for each buffer concentration and peak asymmetry factors
312 were calculated and summarized in **Table 2**. Notably, as the concentration of ammonium
313 acetate increased, the peak tailing of the acyl-CoAs decreased. After evaluating different
314 concentrations of ammonium acetate, a final concentration of 5 mM was chosen, as it resulted
315 in satisfactory peak shapes. Additionally, maintaining a lower salt concentration helps prevent
316 excessive salt precipitation within the instrument, ensuring its proper functionality and
317 longevity. Furthermore, we assessed the influence of pH variation and flow rate on peak tailing
318 but did not observe any significant effects (data not shown). As a result, a flow rate of 0.25
319 mL/min was chosen for chromatographic separation with the presence of 5 mM ammonium
320 acetate in the mobile phases.

321 Further, we tested the effect of cell matrix on peak tailing by spiking four representative acyl-
322 CoA standards in HepG2 cells after extraction. The ammonium acetate concentration of the
323 mobile phase was kept at 5 mM, and peak asymmetry factor was compared between acyl-CoA
324 standards spiked in the cell samples and the standards that were spiked in samples not
325 containing cell matrix. It was observed that peak tailing and subsequently asymmetry factor has
326 been reduced due to the presence of cell matrix (**Figure 2, Table 3**). One possible explanation
327 behind the reduction of peak tailing in the presence of cell matrix is that the components within

328 the cell samples can act as masking agents, thus occupying the tailing sites on the column
329 surface. As a result, the interaction between the acyl-CoA molecules and the column is reduced,
330 leading to a decrease in peak tailing during chromatographic analysis. However, additional
331 investigations are required to confirm this hypothesis. This can also be valuable as
332 understanding the role of the cell matrix in reducing peak tailing can provide valuable insights
333 for optimizing analytical methods and can be helpful in developing strategies to minimize peak
334 tailing and improve the overall performance of chromatographic analyses.

335



337 **Figure 1.** Extracted ion chromatograms of representative acyl-CoA standards (C2:0-CoA,
 338 C8:0-CoA, C16:0-CoA and C18:1-CoA) separated in mobile phases containing 2.5 mM
 339 ammonium acetate (A-D), 5 mM ammonium acetate (E-H) and 10 mM ammonium acetate (I-
 340 L). X-axis represents time (min) and Y-axis represents intensity.

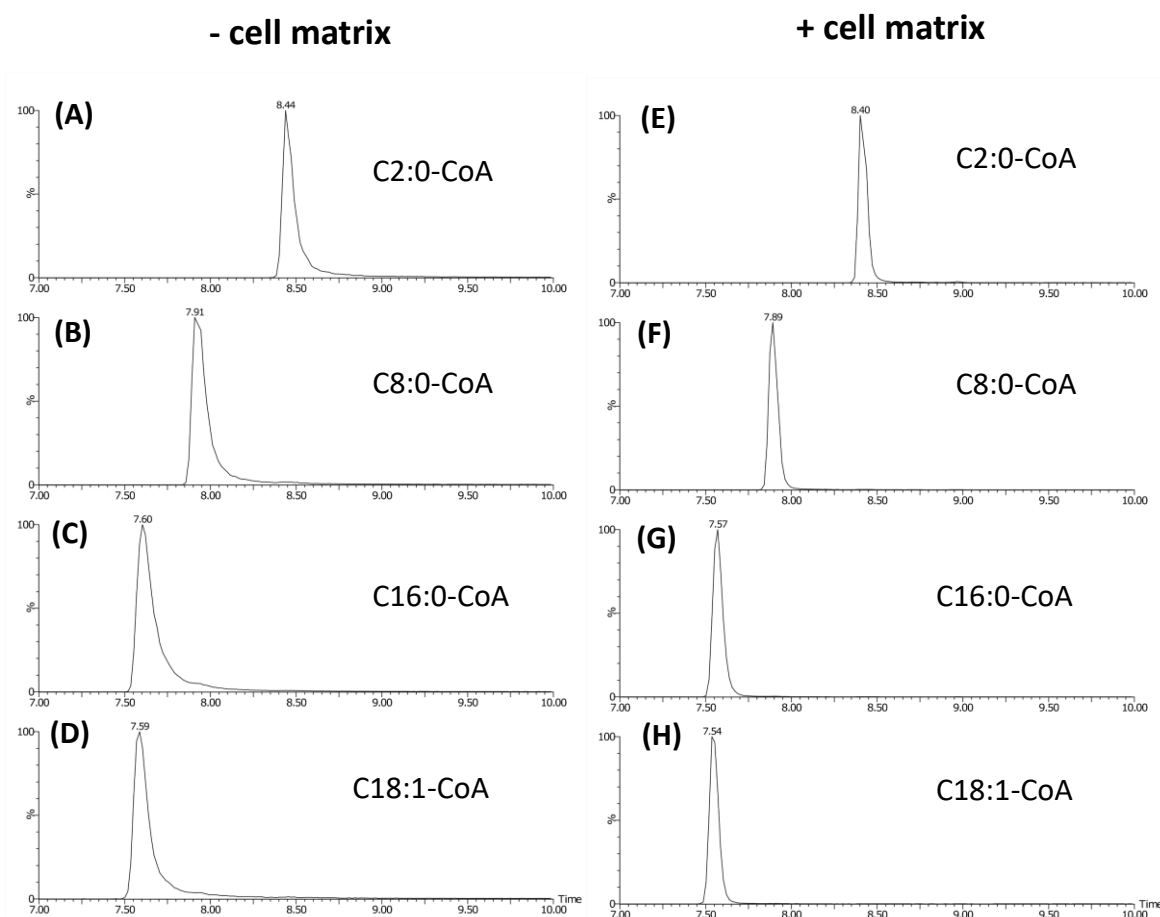
341
 342 **Table 2.** Peak asymmetry factor of acyl-CoA standards with 2.5 mM ammonium acetate, 5 mM
 343 ammonium acetate and 10 mM ammonium acetate.

Concentration of ammonium acetate (mM)	C2:0-CoA	C8:0-CoA	C16:0-CoA	C18:1-CoA
2.5	7.00	5.71	6.38	6.78
5	4.29	3.29	4.38	2.57
10	3.40	2.14	2.57	1.78

344

345

346



347
 348 **Figure 2.** Extracted ion chromatograms of representative acyl-CoA standards (C2:0-CoA,
 349 C8:0-CoA, C16:0-CoA and C18:1-CoA) in 5 mM ammonium acetate, without (A-D) and with
 350 (E-H) cell matrix. X-axis represents time (min) and Y-axis represents intensity.

351

352

353 **Table 3.** Peak asymmetry factor of acyl-CoA standards with and without cell matrix.
354

Cell matrix	C2:0-CoA	C8:0-CoA	C16:0-CoA	C18:1-CoA
Absent (-)	2.32	2.00	3.50	2.28
Present (+)	2.00	1.40	1.33	1.60

355

356 3.3. Optimization of injection solvent for acyl-CoA for sample reconstitution

357 Acyl-CoAs are highly unstable in alkaline and strongly acidic solutions[18]. It is important to
358 check the stability of acyl-CoA in the injection solvents to check for degradation rate and
359 analysis time window. As mentioned previously in literature, methanol was considered to have
360 good stability for acyl-CoA for 24 hours[18]. For this experiment, the four representative acyl-
361 CoA standards (C2:0-CoA, C8:0-CoA, C16:0-CoA and C18:1-CoA) were reconstituted in 5
362 different solutions, MeOH:Water (1:5,v/v), MeOH:Water:IPA (1:1:1,v/v), MeOH:50 mM
363 ammonium acetate (1:1,v/v), MeOH:Water (1:1,v/v) and methanol (100%). The presence of
364 water in the injection solvents is necessary for the solubility of acyl-CoA especially for the
365 short-chain species. The four acyl-CoA standard samples were dissolved in solvents, placed in
366 the autosampler, and analyzed with the HILIC-MS method at three different time points: 0
367 hours, 6 hours, and 24 hours (**Figure 3**).

368 The stability of acyl-CoAs in the various solvents was assessed by measuring the change in
369 response at 6 and 24 hours, expressed as a percentage relative to the response observed at 0
370 hour. Both MeOH:Water (1:5, v/v) and MeOH:Water:IPA (1:1:1, v/v/v) showed acceptable
371 stability over time for the acyl-CoAs. The response with the injection solvent MeOH:50 mM
372 ammonium acetate (1:1,v/v) decreased at 6 and 24 hours, except for C2:0-CoA, which had a
373 higher response at these time points. MeOH:Water (1:1,v/v) and methanol (100%) showed
374 increase in response at 24 hours as compared to 6 hours especially for C2:0-CoA and C8:0-
375 CoA. Methanol (100%) also shows a high variation in response for C2:0-CoA. The exact reason
376 behind this observation is not clearly understood, however, solubility could be one of the
377 contributing factors. For our method, we chose methanol:water:isopropanol (1:1:1,v/v/v) as the
378 injection solvent as it has acceptable stability and the inclusion of slightly less polar solvent
379 (isopropanol) in the injection solvent can increase the solubility of long-chain acyl-CoA.

380

381

382

383

384

385

386

387

388

389

390

391

392

393

394

395

396

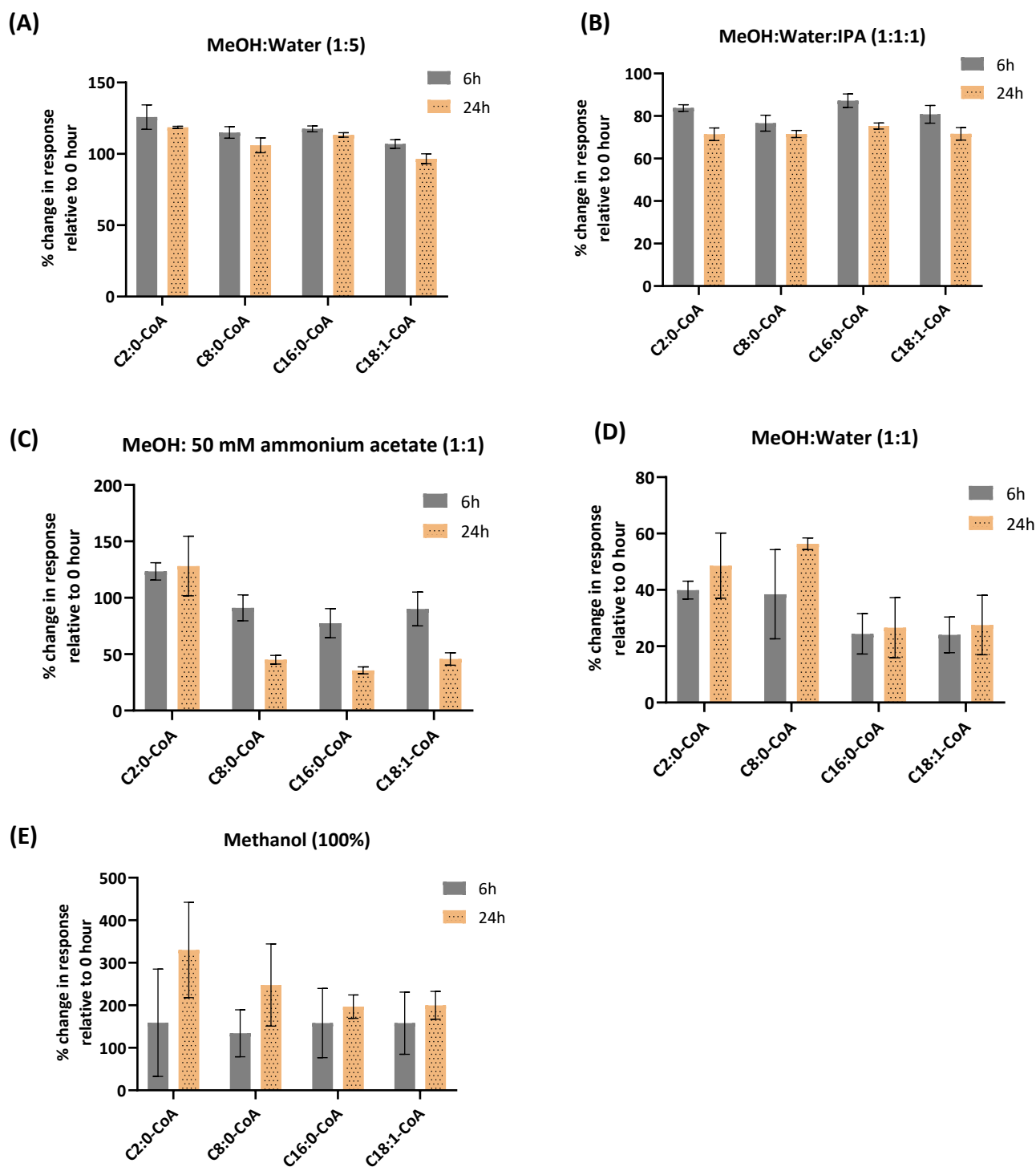
397

398

399

400 **Figure 3.** Stability of representative acyl-CoA standards (C2:0 CoA, C8:0 CoA, C16:0 CoA
 401 and C18:1 CoA) in different injections solvents. (A) MeOH:Water (1:5,v/v); (B)
 402 MeOH:Water:IPA (1:1:1,v/v/v); (C) MeOH:50 mM ammonium acetate (1:1,v/v); (D)
 403 MeOH:Water (1:1,v/v); (E) Methanol (100%).

404



405 3.4. HILIC-MS/MS QTRAP analysis

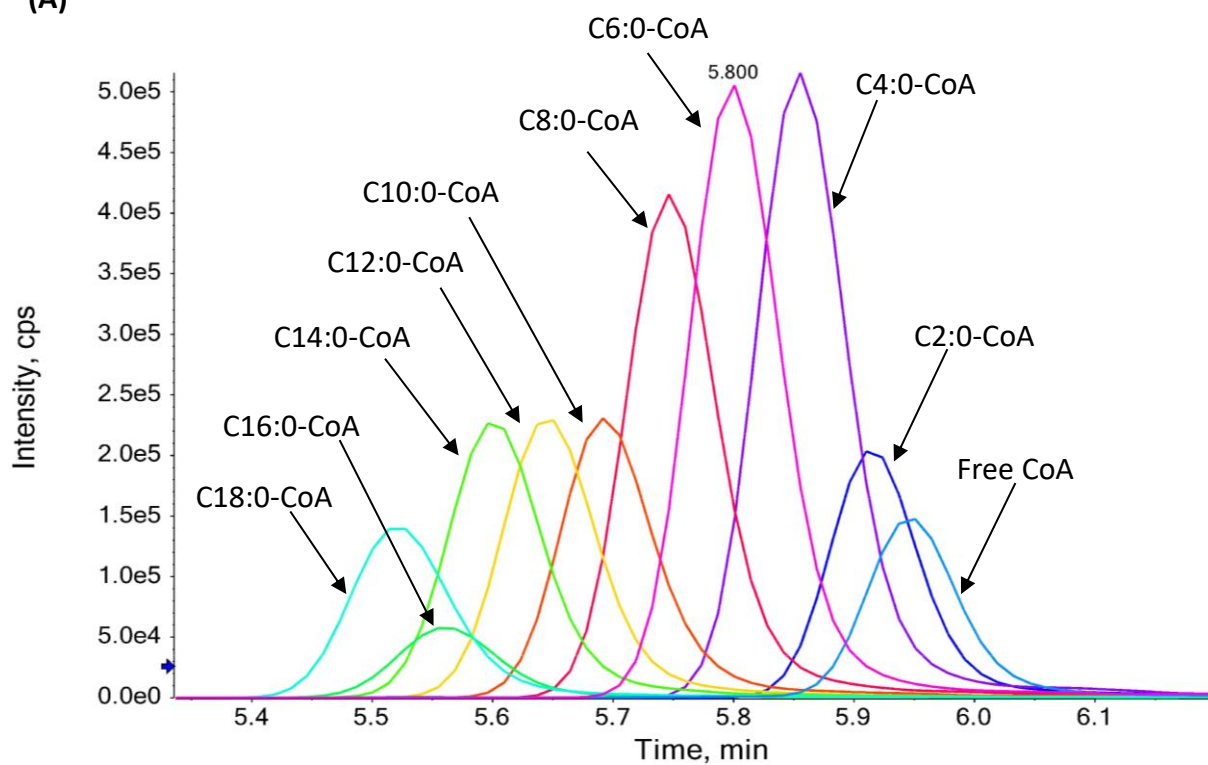
406 Following the optimization of chromatographic and mass spectrometry conditions, a targeted
407 method was created using the sMRM mode on the QTRAP instrument in positive ion mode.
408 We made slight modifications and finalized the gradient as presented in **Table 1**. The formation
409 of water-rich layer on the surface of stationary phase is quite important for interaction with the
410 analytes to ensure consistent retention of compound. Hence, we specifically extended the
411 equilibration time as it is a critical step in HILIC for a stable chromatography. **Figure 4(A)**
412 shows the representative chromatogram of acyl-CoA standards.

413 The fragmentation pattern was examined for the selection of product ion. Acyl-CoA species
414 reveals two important fragments[15,17–19]. The first is the neutral loss of 507 $[M+H-507]^+$,
415 which occurs as a result of the loss of the 3'-phosphate-adenosine-5'-diphosphate moiety from
416 the acyl-CoA precursor molecular ion. Additionally, m/z 428 is another distinctive fragment
417 present in all acyl-CoA species which is the representative CoA moiety. These findings were
418 confirmed in **Figure 4(B)**, which presents the fragmentation pattern of C7:0-CoA. **Figure 4(C)**
419 illustrates the specific site prone to fragmentation of acyl-CoA. The neutral loss of 507 was
420 chosen as the product ion (Q3) for the sMRM mode as it was the most intense and common
421 fragment among acyl-CoAs, as observed in our study and supported by other literatures[15,19].
422 In the HRMS method, the focus was primarily on detecting saturated species, however with the
423 use of highly sensitive QTRAP instrument we were able to detect a few additional
424 monounsaturated species. The confirmation of identification of these monounsaturated species
425 was performed by evaluating their retention time behaviour (**Figure 5**). The intensity of these
426 species was much lower compared to their saturated form, nevertheless their detection can
427 provide additional information and contribute to understanding the biological context of the
428 study samples. The targets along with their sMRM parameters have been mentioned in **Table**
429 **4**.

430

431

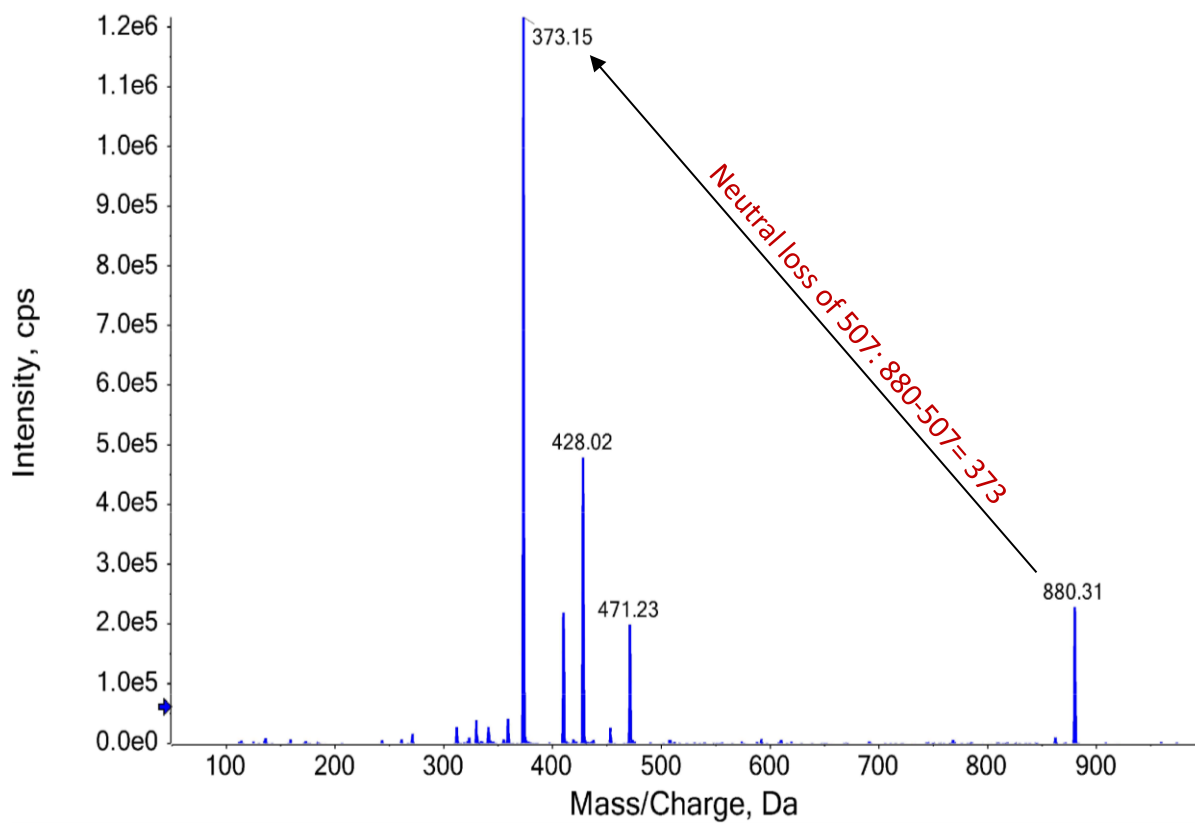
(A)



432

433

(B)



434

435
436
437
438
439
440
441
442
443
444
445
446
447
448

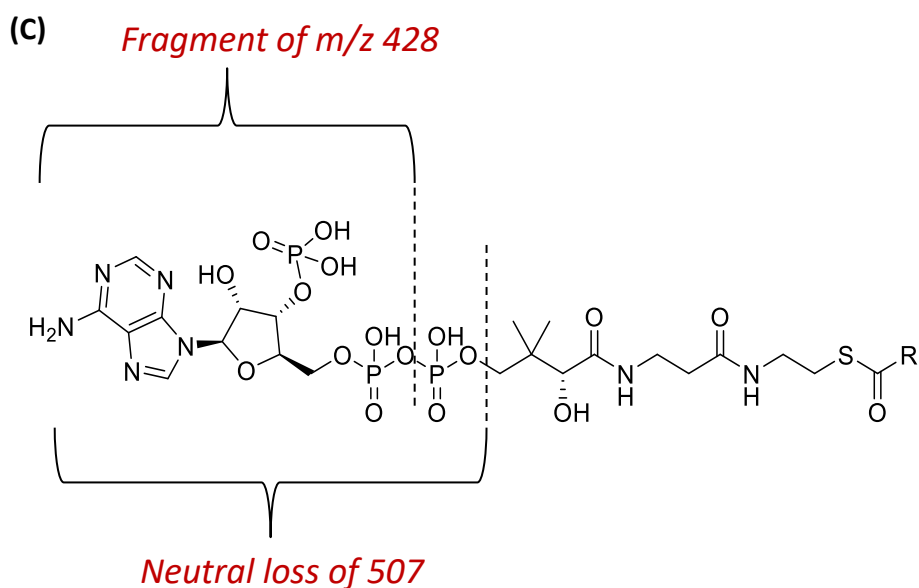


Figure 4. (A) Representative chromatogram of acyl-CoA standards; (B) Mass spectrum showing fragmentation of C7:0-CoA; (C) Structural sites of acyl-CoA fragmentation.

Table 4. sMRM parameters for acyl-CoA targets in HILIC-MS/MS method.

Targets	Q1	Q3	RT	DP	CE
CoA (Free CoA)	768.1	261.1	5.99	100	40
C2:0-CoA (Acetyl-CoA)	810.1	303.1	5.95	100	40
C3:0-CoA (Propionyl-CoA)	824.2	317.2	5.90	100	40
C4:1-CoA	836.2	329.2	ND	100	40
C4:0-CoA	838.2	331.2	5.88	100	40
C6:1-CoA	864.2	357.2	ND	100	40
C6:0-CoA (Hexanoyl-CoA)	866.2	359.2	5.82	100	40
C8:1-CoA	892.2	385.2	5.79	100	40
C8:0-CoA (Octanoyl-CoA)	894.2	387.2	5.76	100	40
C10:1-CoA	920.2	413.2	5.72	100	40
C10:0-CoA (Decanoyl-CoA)	922.3	415.3	5.71	100	40
C12:1-CoA	948.3	441.3	5.68	100	45
C12:0-CoA (Lauroyl-CoA)	950.3	443.3	5.65	100	45
C14:1-CoA	976.3	469.3	5.63	100	45
C14:0-CoA (Myristoyl-CoA)	978.3	471.3	5.61	100	45
C16:1-CoA	1004.3	497.3	5.59	100	45
C16:0-CoA (Palmitoyl-CoA)	1006.4	499.4	5.56	100	45
C18:1-CoA	1032.4	525.4	5.55	100	45
C18:0-CoA (Stearoyl-CoA)	1034.4	527.4	5.54	100	45
C2:0-CoA(¹³ C ₂) (Acetyl-1,2- ¹³ C ₂ -CoA)*	812.1	305.1	5.95	100	40
C7:0-CoA (Heptanoyl-CoA)*	880.2	373.2	5.78	100	40
C15:0-CoA (Pentadecanoyl-CoA)*	992.3	485.3	5.58	100	45

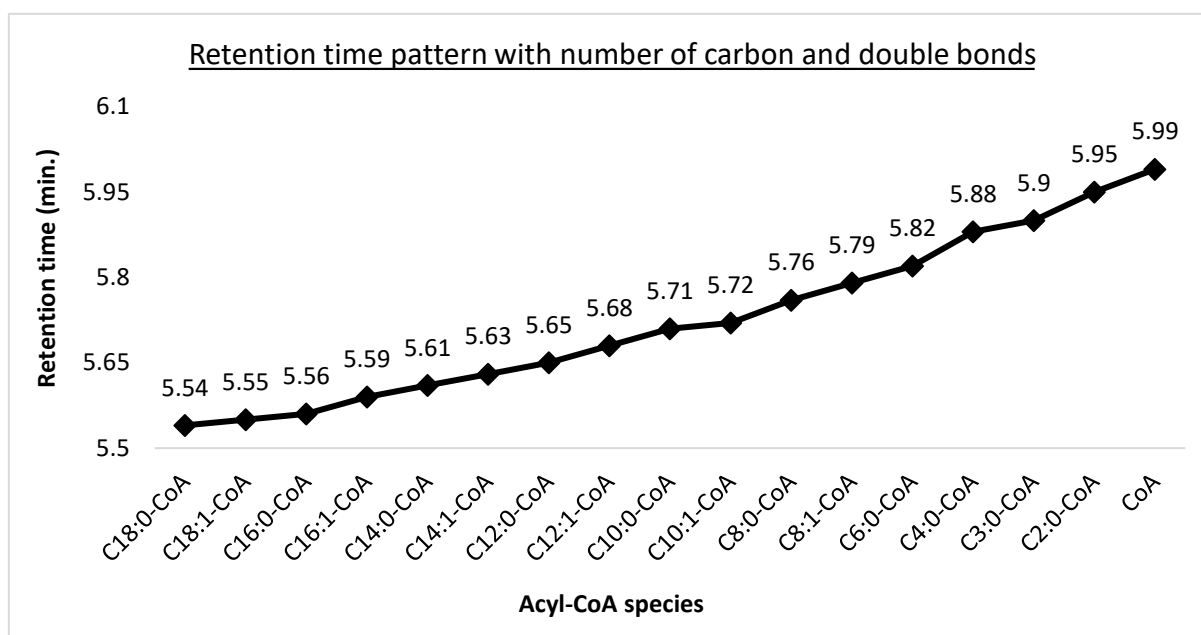
C17:0-CoA (Heptadecanoyl-CoA)*	1020.4	513.4	5.55	100	45
--------------------------------	--------	-------	------	-----	----

449 *, Internal standard; ND, not detected

450

451 3.5. Retention time pattern

452 The identification and confirmation of acyl-CoA species were further supported by analyzing
 453 their retention time pattern. In HILIC chromatography, the gradient initiates with an organic
 454 mobile phase and subsequently transitions to a more aqueous phase. The non-polar nature of a
 455 compound increases with a higher number of carbon chains, whereas the polar character is
 456 intensified by an increase in the number of double bonds. As a result, acyl-CoA species with
 457 longer carbon chains elute first, followed by medium- and short-chain species, as depicted in
 458 **Figure 5**. Similarly, species with a higher number of double bonds but the same number of
 459 carbons elute later compared to species with a lower number of double bonds. For example,
 460 C16:0-CoA elutes at 5.56, while C16:1-CoA elutes at 5.59. This distinct retention time pattern
 461 is highly valuable for the identification and confirmation of a wide range of acyl-CoA species.



462 **Figure 5.** Retention time pattern of acyl-CoA species.

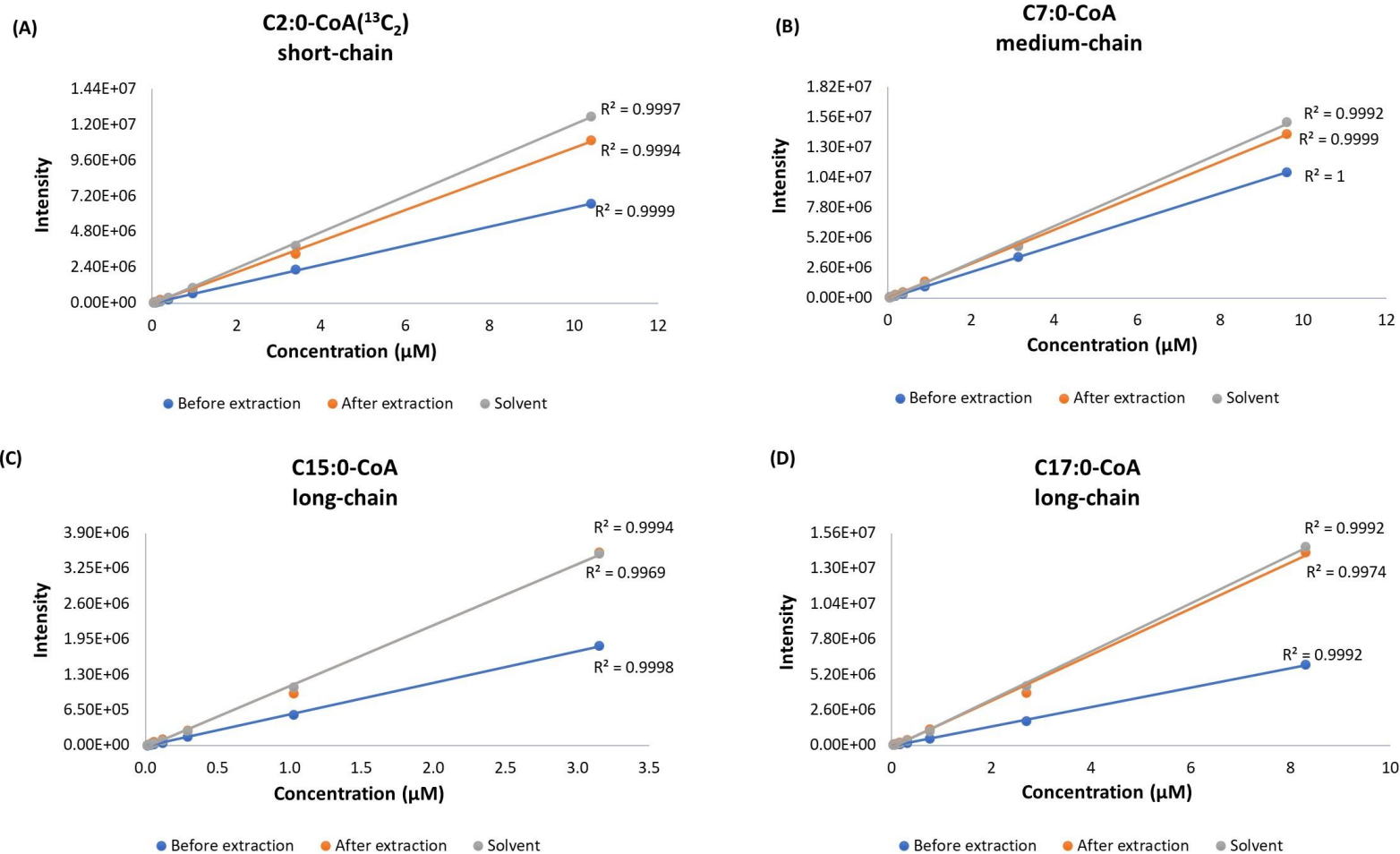
463

464 3.6. Method validation of targeted HILIC-MS/MS method

465 The targeted LC-MS/MS method was validated for quantification of acyl-CoA compounds
 466 spiked in HepG2 cells. Representative non-endogenous standards from short-(C2:0(¹³C₂)-
 467 CoA), medium-(C7:0-CoA) and long-chain (C15:0-CoA and C17:0-CoA) species were chosen
 468 for the validation. The calibration curves of non-endogenous standards spiked in pure solvent

469 and in HepG2 cells (before and after extraction) are shown in **Figure 6**. The values of linearity,
470 LOD, LLOQ, precision, recovery, matrix effect and carryover are reported in **Table 5**. The
471 linear regression coefficients (R^2) were above 0.99 for all spiked standards. The LODs and
472 LLOQs were in the range of (1.3-12.4) pmol mL⁻¹ and (3.1-26.6) pmol mL⁻¹ respectively which
473 makes our method sensitive enough to detect the acyl-CoAs in $\sim 1 \times 10^6$ HepG2 cells. The
474 intraday and interday precisions were determined at low, medium and high concentration levels.
475 Almost all the classes have RSD (%) below 20% except for C15:0 CoA with slightly higher
476 value of 22.9% at low level. The recovery was in the range of (53-123) % for all standards. It
477 was observed that recovery of long-chain acyl-CoA species is slightly lower. The reason for
478 this may be that long-chain acyl-CoA species have lower polarity compared to short- and
479 medium-chain species, which could result in their migration to the non-polar lower layer. The
480 matrix effect was in the range of (85-133)%. The carryover was analyzed in the blank samples
481 placed right after the highest calibration point in HepG2 cells before extraction and was below
482 1% for all standards. We are using non-endogenous compounds as internal standards based on
483 the chain length of endogenous targets. These standards elute in close proximity to the
484 endogenous compounds present in the sample. Hence, the issues related to poor recovery, ion
485 suppression and matrix effects can be compensated as internal standards and endogenous
486 compounds will parallelly go through the same processing.
487 The repeatability evaluates the consistency and reliability of the results, ensuring that there is
488 minimal deviation or variability in the analysis. The repeatability of our HILIC-MS/MS method
489 was determined by measuring the RSD of endogenous acyl-CoA species in QC samples. It was
490 found that out of 19 targets, 7 species show RSD below 5% . The RSD of (5-10) % and (10-15)
491 % was shown by 7 and 1 species respectively while 2 species show RSD in between (15-25)
492 %. Two species were not detected in these samples. In total, 17 acyl-CoA species show RSD
493 below 25% (**Figure S3**).

494
495
496
497
498
499
500
501
502
503
504
505
506



507 **Figure 6.** Calibration curves of non-endogenous acyl-CoA standards spiked in pure solvent, spiked in HepG2 cells before and after extraction. (A)
 508 C2:0-CoA(¹³C₂): short-chain; (B) C7:0-CoA: medium-chain; (C) C15:0-CoA: long-chain; (D) C17:0-CoA: long-chain.

509 **Table 5.** Summary of the validation parameters.

510

Non-endogenous acyl-CoA standards	Linearity	LOD (μM)	LLOQ (μM)	Intraday precision [%]			Interday precision [%]			Recovery [%]			Matrix effect [%]			Carryover [%]
				Low	Medium	High	Low	Medium	High	Low	Medium	High	Low	Medium	High	
C2:0-CoA(¹³C₂)	0.9999	0.0013	0.0031	2.2	2.2	1.0	4.7	3.3	2.5	100.0	88.7	92.2	114.7	101.4	85.7	0.4
C7:0-CoA	1	0.0076	0.0136	4.1	3.4	5.2	12.7	17.4	20.3	123.4	100.1	105.4	124.8	113.0	101.1	0.3
C15:0-CoA	0.9998	0.0110	0.0266	9.5	6.5	4.4	22.9	14.2	11.4	73.1	62.0	80.3	129.9	122.2	89.5	0.3
C17:0-CoA	0.9992	0.0124	0.0230	7.0	5.7	3.0	18.4	6.2	14.1	80.9	53.5	62.5	133.1	113.6	89.0	0.2

511 3.7. Acyl-CoA profile in HepG2 cells cultured in supplemented and starved state

512 We applied our HILIC-MS/MS method to analyze acyl-CoA profile of wildtype HepG2 cells
513 cultured under two different conditions. In Condition 1 (supplemented cells), the cells were
514 cultured in a medium containing glucose, pyruvate, glutamine with supplementation of
515 carnitine and palmitate. On the other hand, Condition 2 (starved cells) involved culturing the
516 cells in a glucose-free medium with no pyruvate and glutamine, but with the addition of
517 carnitine and palmitate, aiming to simulate a state of starvation. **Figure 7(A)** shows the profile
518 of free CoA and short- to long-chain acyl-CoAs in HepG2 cells cultured under both
519 supplemented (condition 1) and starved conditions (condition 2). **Figure 7(B)** displays the fold
520 change in acyl-CoA levels between the supplemented and starved states. We observed a
521 decrease in the free CoA level ($p < 0.05$) during the starvation state of HepG2 cells while there
522 has been an increase in the acetyl-CoA ($p < 0.0001$) in starved cells as compared to
523 supplemented ones. The medium chain acyl-CoA also showed an increase in their profile in
524 starved conditions for C6:0-CoA ($p < 0.0021$), C8:0-CoA ($p < 0.05$) and C10:0-CoA ($p < 0.0002$).
525 Furthermore, we observed an increase in the profile of long-chain acyl-CoA such as C12:0-
526 CoA, C14:0-CoA and C16:0-CoA with $p < 0.0001$.

527 The change in the profile of acyl-CoA in our study shows an activation of fatty acid oxidation.
528 During starvation conditions, cells shift in the survival mode due to decrease in glucose level,
529 activating the FAO process. In FAO, free fatty acids are activated to long-chain acyl-CoA and
530 enter inside the mitochondria for fatty acid oxidation process, thus leading to an increase in the
531 level of long-chain acyl-CoA. A study has reported an increase in the expression of acyl-CoA
532 synthetase (ACS) and carnitine palmitoyltransferase-1 (CPT-1) while decrease in the level of
533 acetyl-CoA carboxylase (ACC) during fasting conditions[45]. ACS increases the formation of
534 fatty acyl-CoA from fatty acid and CPT-1 is responsible for converting acyl-CoAs into
535 acylcarnitines. The increase in the level of both of these enzymes suggests an increase in the
536 transportation of long-chain acyl-CoA inside mitochondria. Our data also reflects the same with
537 increase in the profile of long-chain acyl-CoAs in the starved state. On the contrary, ACC
538 controls the rate limiting step of FAO by facilitating the formation of malonyl-CoA, an inhibitor
539 of CPT-1. The decrease in its level further supports the formation of long-chain acyl-CoA.
540 Acetyl-CoA (C2:0-CoA) is the final product of the FAO pathway. We observed an increase in
541 acetyl-CoA levels, indicating an activation of the FAO pathway. This increased acetyl-CoA
542 formation supports ATP synthesis and promotes the production of ketone bodies[46]. The
543 activation of FAO relative to downstream Krebs cycle and oxidative phosphorylation, further
544 contributes to the accumulation of acetyl-CoA during the state of starvation.

545 Our observations also indicate decrease in the profile of free CoA during starvation conditions.
546 One hypothesis to support this observation is an increased utilization of CoA for fatty acid
547 activation by formation of acyl-CoA esters and subsequent FAO processes. This reduction in
548 free CoA levels can be associated with the higher demand for acyl-CoA formation due to the
549 observed increase of acyl-CoA thioesters in our study. Another possible hypothesis could be
550 the inhibition of pantothenate kinase, an enzyme responsible for catalyzing the initial
551 biosynthetic step of free CoA. It is known that higher concentrations of long-chain acyl-CoA
552 and acetyl-CoA can inhibit this enzyme[47]. Consequently, this inhibition of pantothenate
553 kinase may also contribute to the decrease in CoA biosynthesis and subsequently lead to a
554 reduction in free CoA levels.

555

556

557

558

559

560

561

562

(A)

563

564

565

566

567

568

569

570

571

572

573

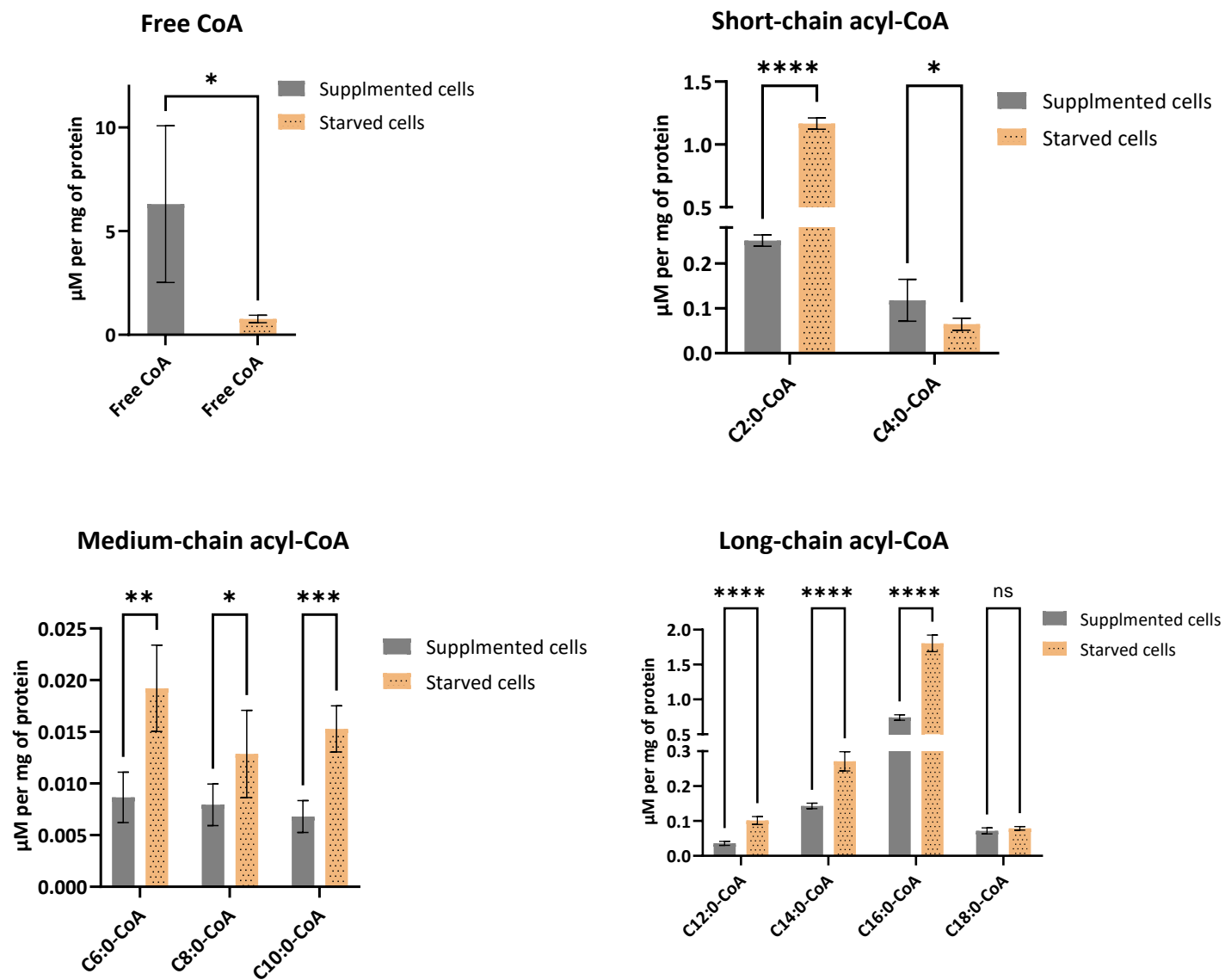
574

575

576

577

578



579

(B)

580

581

582

583

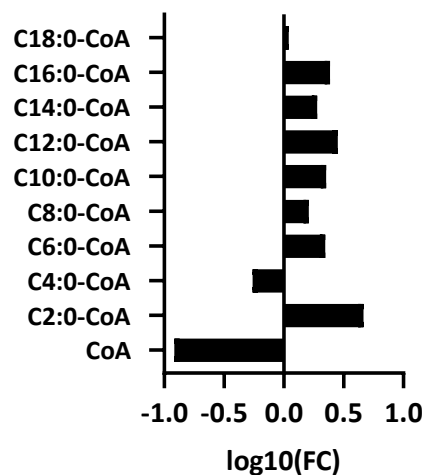
584

585

586

587

Fold change (Starved/Supplemented)



588

589

590

591

592

593

594

595

Figure 7. Acyl-CoAs profile in supplemented vs starved conditions in wildtype HepG2 cells.(A) Bar graph showing concentration of free CoA, short-chain acyl-CoA; medium-chain acyl-CoA and long-chain acyl-CoA in supplemented and starved state.(* $p < 0.05$; ** $p < 0.0021$; *** $p < 0.0002$; **** $p < 0.0001$; ns, not significant). (B) Fold change of acyl-CoAs in starved/supplemented conditions.

596 4. Conclusion

597 We have developed a HILIC-MS/MS method utilizing a zwitterionic ZIC-cHILIC column,
598 covering short- to long-chain acyl-CoA species in one analytical run with the use of lower
599 concentration of ammonium acetate. This HILIC-MS/MS method was assessed on various
600 validation parameters and was applied to evaluate the change in acyl-CoA profile in wildtype
601 HepG2 cells cultured in supplemented and starved state. We observed an increase in the profile
602 of acetyl-CoA, medium- and long-chain acyl-CoA while decrease in the level of free CoA in
603 HepG2 cells cultured in starved state. These findings suggest an increase in the fatty acid
604 oxidation process in starved state, relative to the downstream metabolic processes.

605 The comprehensive analysis of acyl-CoA species in one run is highly beneficial for high-
606 throughput analysis of biological samples and has the potential of integration in clinical settings.
607 This HILIC-MS/MS method can be further extended in future to cover very long-chain acyl-
608 CoA species. However, separation and identification of isomers such butyryl and isobutyryl-
609 CoA, succinyl-CoA and methylmalonyl-CoA etc., or the identification of position of double
610 bond in species such C10:1-CoA or C18:1-CoA is the limitation associated with this method
611 and therefore, these species were reported by the carbon chain composition instead of their
612 names. Hence, in future further investigation should be performed for the separation of these
613 isomeric species.

614 **CRedit authorship contribution statement**

616 Madhulika Singh: Investigation, Conceptualization, Methodology, Data curation,
617 Visualization, Writing – original draft & editing. Ligia Akemi Kiyuna: Methodology,
618 Investigation, Writing – review & editing. Christoff Odendaal: Methodology, Writing – review
619 & editing. Barbara Bakker: Writing – review & editing. Amy Harms: Supervision, Writing –
620 review & editing. Thomas Hankemeier: Supervision, Funding acquisition, Writing – review &
621 editing.

622 **Declaration of Competing Interest**

624 The authors declare no competing financial interest.

625 **Acknowledgements**

626 This work was supported by the European Union's Horizon 2020 research and innovation
627 program under the Marie Skłodowska-Curie grant agreement PoLiMeR, No 812616; the Dutch
628 Research Council (NWO) 'Investment Grant NWO Large' program, for the 'Building the

629 infrastructure for Exposome research: Exposome-Scan' [No. 175.2019.032]; the NWO
630 Netherlands X-omics Initiative [No. 184.034.019]; EXPOSOME-NL, which is funded through
631 the Gravitation program of the Dutch Ministry of Education, Culture, and Science and the
632 Netherlands Organization for Scientific Research (NWO grant number 024.004.017).
633 The authors also acknowledge Asmara Drachman, Vladka Cetkovska and Gaby Liem Foeng
634 Kioen for their technical assistance.

635 **Data availability**

636
637 Data will be made available on request
638

639

640 **Appendix A. Supplementary data**

641
642
643
644
645
646

647 **References**

- 648
- 649 [1] C.C.C.R. de Carvalho, M.J. Caramujo, The Various Roles of Fatty Acids, *Molecules*. 23
650 (2018) 2583. <https://doi.org/10.3390/molecules23102583>.
 - 651 [2] E.P. Brass, Overview of coenzyme A metabolism and its role in cellular toxicity,
652 *Chemico-Biological Interactions*. 90 (1994) 203–214. [https://doi.org/10.1016/0009-](https://doi.org/10.1016/0009-2797(94)90010-8)
653 [2797\(94\)90010-8](https://doi.org/10.1016/0009-2797(94)90010-8).
 - 654 [3] J.L. Merritt, E. MacLeod, A. Jurecka, B. Hainline, Clinical manifestations and
655 management of fatty acid oxidation disorders, *Rev Endocr Metab Disord*. 21 (2020)
656 479–493. <https://doi.org/10.1007/s11154-020-09568-3>.
 - 657 [4] S.M. Houten, R.J.A. Wanders, A general introduction to the biochemistry of
658 mitochondrial fatty acid β -oxidation, *J Inherit Metab Dis*. 33 (2010) 469–477.
659 <https://doi.org/10.1007/s10545-010-9061-2>.
 - 660 [5] P.A. Watkins, Fatty acid activation, *Prog Lipid Res*. 36 (1997) 55–83.
661 [https://doi.org/10.1016/s0163-7827\(97\)00004-0](https://doi.org/10.1016/s0163-7827(97)00004-0).
 - 662 [6] J.M. Ellis, C.E. Bowman, M.J. Wolfgang, Metabolic and Tissue-Specific Regulation of
663 Acyl-CoA Metabolism, *PLOS ONE*. 10 (2015) e0116587.
664 <https://doi.org/10.1371/journal.pone.0116587>.
 - 665 [7] Q. Li, S. Zhang, J.M. Berthiaume, B. Simons, G.-F. Zhang, Novel approach in LC-
666 MS/MS using MRM to generate a full profile of acyl-CoAs: discovery of acyl-
667 dephospho-CoAs, *J Lipid Res*. 55 (2014) 592–602. <https://doi.org/10.1194/jlr.D045112>.
 - 668 [8] T.J. Grevengoed, E.L. Klett, R.A. Coleman, Acyl-CoA Metabolism and Partitioning,
669 *Annu Rev Nutr*. 34 (2014) 1–30. <https://doi.org/10.1146/annurev-nutr-071813-105541>.
 - 670 [9] T. Migita, K. Takayama, T. Urano, D. Obinata, K. Ikeda, T. Soga, S. Takahashi, S.
671 Inoue, ACSL3 promotes intratumoral steroidogenesis in prostate cancer cells, *Cancer*
672 *Sci*. 108 (2017) 2011–2021. <https://doi.org/10.1111/cas.13339>.

- 673 [10] S. Zhang, O.D. Nelson, I.R. Price, C. Zhu, X. Lu, I.R. Fernandez, R.S. Weiss, H. Lin,
674 Long-chain fatty acyl coenzyme A inhibits NME1/2 and regulates cancer metastasis,
675 Proceedings of the National Academy of Sciences. 119 (2022) e2117013119.
676 <https://doi.org/10.1073/pnas.2117013119>.
- 677 [11] S. Jackowski, R. Leonardi, Deregulated Coenzyme A, Loss of Metabolic Flexibility and
678 Diabetes, *Biochem Soc Trans.* 42 (2014) 1118–1122.
679 <https://doi.org/10.1042/BST20140156>.
- 680 [12] J.E. Kanter, F. Kramer, S. Barnhart, M.M. Averill, A. Vivekanandan-Giri, T. Vickery,
681 L.O. Li, L. Becker, W. Yuan, A. Chait, K.R. Braun, S. Potter-Perigo, S. Sanda, T.N.
682 Wight, S. Pennathur, C.N. Serhan, J.W. Heinecke, R.A. Coleman, K.E. Bornfeldt,
683 Diabetes promotes an inflammatory macrophage phenotype and atherosclerosis through
684 acyl-CoA synthetase 1, Proceedings of the National Academy of Sciences. 109 (2012)
685 E715–E724. <https://doi.org/10.1073/pnas.1111600109>.
- 686 [13] A. Michno, A. Raszeja-Specht, A. Jankowska-Kulawy, T. Pawelczyk, A. Szutowicz,
687 Effect of L-Carnitine on Acetyl-CoA Content and Activity of Blood Platelets in Healthy
688 and Diabetic Persons, *Clinical Chemistry.* 51 (2005) 1673–82.
689 <https://doi.org/10.1373/clinchem.2005.050328>.
- 690 [14] S. HORIE, M. ISOBE, T. SUGA, Changes in CoA Pools in Hepatic Peroxisomes of the
691 Rat, under Various Conditions, *The Journal of Biochemistry.* 99 (1986) 1345–1352.
692 <https://doi.org/10.1093/oxfordjournals.jbchem.a135602>.
- 693 [15] P. Li, M. Gawaz, M. Chatterjee, M. Lämmerhofer, Targeted Profiling of Short-,
694 Medium-, and Long-Chain Fatty Acyl-Coenzyme As in Biological Samples by
695 Phosphate Methylation Coupled to Liquid Chromatography–Tandem Mass
696 Spectrometry, *Anal. Chem.* 93 (2021) 4342–4350.
697 <https://doi.org/10.1021/acs.analchem.1c00664>.
- 698 [16] L. Gao, W. Chiou, H. Tang, X. Cheng, H. Camp, D. Burns, Simultaneous quantification
699 of malonyl-CoA and several other short-chain acyl-CoAs in animal tissues by ion-
700 pairing reversed-phase HPLC/MS, *Journal of Chromatography. B, Analytical*
701 *Technologies in the Biomedical and Life Sciences.* 853 (2007) 303–13.
702 <https://doi.org/10.1016/j.jchromb.2007.03.029>.
- 703 [17] S. Wang, Z. Wang, L. Zhou, X. Shi, G. Xu, Comprehensive Analysis of Short-,
704 Medium-, and Long-Chain Acyl-Coenzyme A by Online Two-Dimensional Liquid
705 Chromatography/Mass Spectrometry, *Anal. Chem.* 89 (2017) 12902–12908.
706 <https://doi.org/10.1021/acs.analchem.7b03659>.
- 707 [18] X. Yang, Y. Ma, N. Li, H. Cai, M.G. Bartlett, Development of a Method for the
708 Determination of Acyl-CoA Compounds by Liquid Chromatography Mass Spectrometry
709 to Probe the Metabolism of Fatty Acids, *Anal. Chem.* 89 (2017) 813–821.
710 <https://doi.org/10.1021/acs.analchem.6b03623>.
- 711 [19] L.G. Rivera, M.G. Bartlett, Chromatographic methods for the determination of acyl-
712 CoAs, *Anal. Methods.* 10 (2018) 5252–5264. <https://doi.org/10.1039/C8AY01472H>.
- 713 [20] P.G. Tardi, J.J. Mukherjee, P.C. Choy, The quantitation of long-chain acyl-CoA in
714 mammalian tissue, *Lipids.* 27 (1992) 65–67. <https://doi.org/10.1007/BF02537062>.
- 715 [21] G. Liu, J. Chen, P. Che, Y. Ma, Separation and Quantitation of Short-Chain Coenzyme
716 A's in Biological Samples by Capillary Electrophoresis, *Anal. Chem.* 75 (2003) 78–82.
717 <https://doi.org/10.1021/ac0261505>.
- 718 [22] A. Demoz, A. Garras, D.K. Asiedu, B. Nettelnd, R.K. Berge, Rapid method for the
719 separation and detection of tissue short-chain coenzyme A esters by reversed-phase
720 high-performance liquid chromatography, *Journal of Chromatography B: Biomedical*
721 *Sciences and Applications.* 667 (1995) 148–152. [https://doi.org/10.1016/0378-](https://doi.org/10.1016/0378-4347(94)00595-V)
722 [4347\(94\)00595-V](https://doi.org/10.1016/0378-4347(94)00595-V).

- 723 [23] L. Abrankó, G. Williamson, S. Gardner, A. Kerimi, Comprehensive quantitative analysis
724 of fatty-acyl-Coenzyme A species in biological samples by ultra-high performance
725 liquid chromatography–tandem mass spectrometry harmonizing hydrophilic interaction
726 and reversed phase chromatography, *Journal of Chromatography A*. 1534 (2018) 111–
727 122. <https://doi.org/10.1016/j.chroma.2017.12.052>.
- 728 [24] N.W. Snyder, S.S. Basu, Z. Zhou, A.J. Worth, I.A. Blair, Stable isotope dilution liquid
729 chromatography-mass spectrometry analysis of cellular and tissue medium- and long-
730 chain acyl-coenzyme A thioesters, *Rapid Commun Mass Spectrom*. 28 (2014) 1840–
731 1848. <https://doi.org/10.1002/rcm.6958>.
- 732 [25] S.M. Lam, T. Zhou, J. Li, S. Zhang, G.H. Chua, B. Li, G. Shui, A robust, integrated
733 platform for comprehensive analyses of acyl-coenzyme As and acyl-carnitines revealed
734 chain length-dependent disparity in fatty acyl metabolic fates across *Drosophila*
735 development, *Science Bulletin*. 65 (2020) 1840–1848.
736 <https://doi.org/10.1016/j.scib.2020.07.023>.
- 737 [26] A.E. Jones, N.J. Arias, A. Acevedo, S.T. Reddy, A.S. Divakaruni, D. Meriwether, A
738 Single LC-MS/MS Analysis to Quantify CoA Biosynthetic Intermediates and Short-
739 Chain Acyl CoAs, *Metabolites*. 11 (2021) 468. <https://doi.org/10.3390/metabo11080468>.
- 740 [27] M. Holcapek, K. Volná, P. Jandera, L. Kolářová, K. Lemr, M. Exner, A. Církva, Effects
741 of ion-pairing reagents on the electrospray signal suppression of sulphonated dyes and
742 intermediates, *J Mass Spectrom*. 39 (2004) 43–50. <https://doi.org/10.1002/jms.551>.
- 743 [28] B. Buszewski, S. Noga, Hydrophilic interaction liquid chromatography (HILIC)--a
744 powerful separation technique, *Anal Bioanal Chem*. 402 (2012) 231–247.
745 <https://doi.org/10.1007/s00216-011-5308-5>.
- 746 [29] R. Li, J. Huang, Chromatographic behavior of epirubicin and its analogues on high-
747 purity silica in hydrophilic interaction chromatography, *J Chromatogr A*. 1041 (2004)
748 163–169. <https://doi.org/10.1016/j.chroma.2004.04.033>.
- 749 [30] P. Hemström, K. Irgum, Hydrophilic interaction chromatography, *Journal of Separation*
750 *Science*. 29 (2006) 1784–1821. <https://doi.org/10.1002/jssc.200600199>.
- 751 [31] H. Wu, A.D. Southam, A. Hines, M.R. Viant, High-throughput tissue extraction protocol
752 for NMR- and MS-based metabolomics, *Anal Biochem*. 372 (2008) 204–212.
753 <https://doi.org/10.1016/j.ab.2007.10.002>.
- 754 [32] T. Van Der Laan, A.-C. Dubbelman, K. Duisters, A. Kindt, A.C. Harms, T. Hankemeier,
755 High-Throughput Fractionation Coupled to Mass Spectrometry for Improved
756 Quantitation in Metabolomics, *Anal. Chem*. 92 (2020) 14330–14338.
757 <https://doi.org/10.1021/acs.analchem.0c01375>.
- 758 [33] N. Kadian, K.S.R. Raju, M. Rashid, M.Y. Malik, I. Taneja, M. Wahajuddin,
759 Comparative assessment of bioanalytical method validation guidelines for
760 pharmaceutical industry, *Journal of Pharmaceutical and Biomedical Analysis*. 126
761 (2016) 83–97. <https://doi.org/10.1016/j.jpba.2016.03.052>.
- 762 [34] D. Wolrab, M. Chocholoušková, R. Jirásko, O. Peterka, M. Holcapek, Validation of
763 lipidomic analysis of human plasma and serum by supercritical fluid chromatography-
764 mass spectrometry and hydrophilic interaction liquid chromatography-mass
765 spectrometry, *Anal Bioanal Chem*. 412 (2020) 2375–2388.
766 <https://doi.org/10.1007/s00216-020-02473-3>.
- 767 [35] M. Azim, M. Moloy, P. Bhasin, HPLC METHOD DEVELOPMENT AND
768 VALIDATION: A REVIEW, *International Research Journal of Pharmacy*. 4 (2015) 39–
769 46. <https://doi.org/10.7897/2230-8407.04407>.
- 770 [36] merck_sequant-zic-chilic_brochure.pdf, (n.d.). [https://mz-](https://mz-at.de/fileadmin/user_upload/Brochures/merck_sequant-zic-chilic_brochure.pdf)
771 [at.de/fileadmin/user_upload/Brochures/merck_sequant-zic-chilic_brochure.pdf](https://mz-at.de/fileadmin/user_upload/Brochures/merck_sequant-zic-chilic_brochure.pdf) (accessed
772 June 8, 2023).

- 773 [37] F. Hosseinkhani, L. Huang, A.-C. Dubbelman, F. Guled, A.C. Harms, T. Hankemeier,
774 Systematic Evaluation of HILIC Stationary Phases for Global Metabolomics of Human
775 Plasma, *Metabolites*. 12 (2022) 165. <https://doi.org/10.3390/metabo12020165>.
- 776 [38] S. Arase, S. Kimura, T. Ikegami, Method optimization of hydrophilic interaction
777 chromatography separation of nucleotides using design of experiment approaches I:
778 Comparison of several zwitterionic columns, *J Pharm Biomed Anal*. 158 (2018) 307–
779 316. <https://doi.org/10.1016/j.jpba.2018.05.014>.
- 780 [39] E. Zborníková, Z. Knejzlík, V. Hauryliuk, L. Krásný, D. Rejman, Analysis of nucleotide
781 pools in bacteria using HPLC-MS in HILIC mode, *Talanta*. 205 (2019) 120161.
782 <https://doi.org/10.1016/j.talanta.2019.120161>.
- 783 [40] A. Wakamatsu, K. Morimoto, M. Shimizu, S. Kudoh, A severe peak tailing of phosphate
784 compounds caused by interaction with stainless steel used for liquid chromatography and
785 electrospray mass spectrometry, *Journal of Separation Science*. 28 (2005) 1823–1830.
786 <https://doi.org/10.1002/jssc.200400027>.
- 787 [41] H.-L. Koh, A.-J. Lau, E.C.-Y. Chan, Hydrophilic interaction liquid chromatography with
788 tandem mass spectrometry for the determination of underivatized dencichine (beta-N-
789 oxalyl-L-alpha,beta-diaminopropionic acid) in Panax medicinal plant species, *Rapid*
790 *Commun Mass Spectrom*. 19 (2005) 1237–1244. <https://doi.org/10.1002/rcm.1928>.
- 791 [42] I. Kohler, M. Verhoeven, R. Haselberg, A.F.G. Gargano, Hydrophilic interaction
792 chromatography – mass spectrometry for metabolomics and proteomics: state-of-the-art
793 and current trends, *Microchemical Journal*. 175 (2022) 106986.
794 <https://doi.org/10.1016/j.microc.2021.106986>.
- 795 [43] Y. Du, Y. Li, X. Hu, X. Deng, Z. Qian, Z. Li, M. Guo, D. Tang, Development and
796 evaluation of a hydrophilic interaction liquid chromatography-MS/MS method to
797 quantify 19 nucleobases and nucleosides in rat plasma, *Biomedical Chromatography*. 31
798 (2017) e3860. <https://doi.org/10.1002/bmc.3860>.
- 799 [44] X. Liu, Z. Ser, J.W. Locasale, Development and Quantitative Evaluation of a High-
800 Resolution Metabolomics Technology, *Anal. Chem*. 86 (2014) 2175–2184.
801 <https://doi.org/10.1021/ac403845u>.
- 802 [45] M.-H. Ryu, J.W. Daily, Y.-S. Cha, Effect of starvation on hepatic acyl-CoA synthetase,
803 carnitine palmitoyltransferase-I, and acetyl-CoA carboxylase mRNA levels in rats,
804 *Nutrition*. 21 (2005) 537–542. <https://doi.org/10.1016/j.nut.2004.08.015>.
- 805 [46] L. Shi, B.P. Tu, Acetyl-CoA and the Regulation of Metabolism: Mechanisms and
806 Consequences, *Curr Opin Cell Biol*. 33 (2015) 125–131.
807 <https://doi.org/10.1016/j.ceb.2015.02.003>.
- 808 [47] Y.-M. Zhang, C.O. Rock, S. Jackowski, Feedback Regulation of Murine Pantothenate
809 Kinase 3 by Coenzyme A and Coenzyme A Thioesters, *Journal of Biological Chemistry*.
810 280 (2005) 32594–32601. <https://doi.org/10.1074/jbc.M506275200>.
- 811